ACS Medicinal Chemistry Letters

pubs.acs.org/acsmedchemlett Letter

Discovery of DS79932728: A Potent, Orally Available G9a/GLP Inhibitor for Treating β-Thalassemia and Sickle Cell Disease

Katsushi Katayama,* Ken Ishii, Hideki Terashima, Eisuke Tsuda, Makoto Suzuki, Keiichi Yotsumoto, Kumiko Hiramoto, Isao Yasumatsu, Munefumi Torihata, Takashi Ishiyama, Tsuyoshi Muto, and Takahiro Katagiri*

Cite This: *ACS Med. Chem. Lett.* 2021, 12, 121−128 Read Online

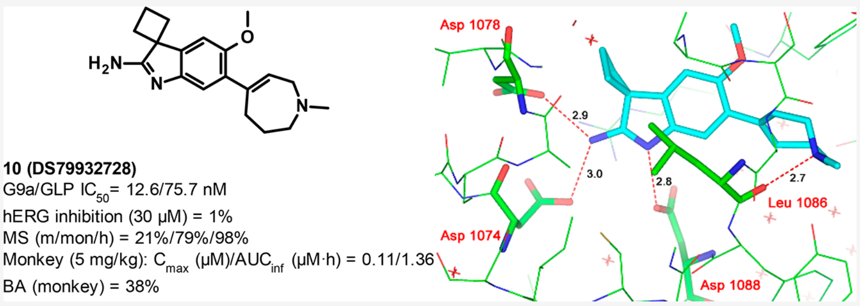

ABSTRACT: Therapeutic reactivation of the γ-globin genes for fetal hemoglobin (HbF) production is an attractive strategy for treating β-thalassemia and sickle cell disease. It was reported that genetic knockdown of the histone lysine methyltransferase EHMT2/1 (G9a/GLP) is sufficient to induce HbF production. The aim of the present work was to acquire a G9a/GLP inhibitor that induces HbF production sufficiently. It was revealed that tetrahydroazepine has versatility as a side chain in various skeletons. We ultimately obtained a promising aminoindole derivative (DS79932728), a potent and orally bioavailable G9a/GLP inhibitor that was found to induce γ-globin production in a phlebotomized cynomolgus monkey model. This work could facilitate the development of effective new approaches for treating β-thalassemia and sickle cell disease.

KEYWORDS: *fetal hemoglobin, histone lysine methyltransferase, EHMT1/2, G9a/GLP, epigenetics, tetrahydroazepine*

β-Thalassemia and sickle cell disease (SCD) are recessive hemoglobinopathies that affect the structure and production of hemoglobin, specifically β-globin.[1] β-Thalassemia is caused by a diverse range of genetic changes that lead to the reduced production of β-globin and insufficiently hemoglobinized red blood cells (RBCs).[2] In SCD, a β-globin gene substitution ($\beta^{6\mathrm{Glu}\rightarrow\mathrm{Val}}$) causes sickle hemoglobin (HbS; $\alpha 2\beta^{s}2$) in a deoxygenated state, resulting in hemolysis and vaso-occlusion.[3] Patients with severe hemoglobinopathies require regular blood transfusions to survive, but these, in turn, may result in life-threatening complications, such as iron overload.[4]

Adult hemoglobin (HbA; $\alpha 2\beta 2$), which is responsible for carrying oxygen in adult blood, consists of heterotetramers composed of two α-globins and two β-globins. During fetal development, however, erythrocytes preferentially express an alternative hemoglobin tetramer called fetal hemoglobin (HbF; $\alpha 2\gamma 2$), which is composed of two α-globins and two γ-globins instead of β-globin chains. Several months after birth, the transition from HbF to HbA occurs through a process called globin switching.[5] Clinical studies have shown that increased HbF production in RBCs leads to the amelioration of the disease progression of β-thalassemia and SCD, so therapeutic agents that increase HbF production have become an important therapeutic strategy for reducing clinical morbidity and mortality in patients with hemoglobinopathies.[6] Hydroxyurea (HU), with its proven efficacy in reducing sickle cell crises and improving survival, was the first drug approved by the Food and Drug Administration (FDA) for the treatment of SCD.[7] Although HU treatment can induce HbF production and reduce the suffering of patients with SCD, there are important limitations to its clinical utility due to its low efficacy, several adverse effects, and inability to elicit a response in all patients.[8,9] Very recently, voxelotor (Oxbryta), a HbS polymerization inhibitor, was approved by the FDA for the treatment of SCD. This first-in-class therapy enhances the affinity of hemoglobin for oxygen, resulting in decreased deoxygenated HbS and hemoglobin polymerization to counter RBC destruction.[10] In

Received: October 28, 2020
Accepted: December 21, 2020
Published: December 28, 2020

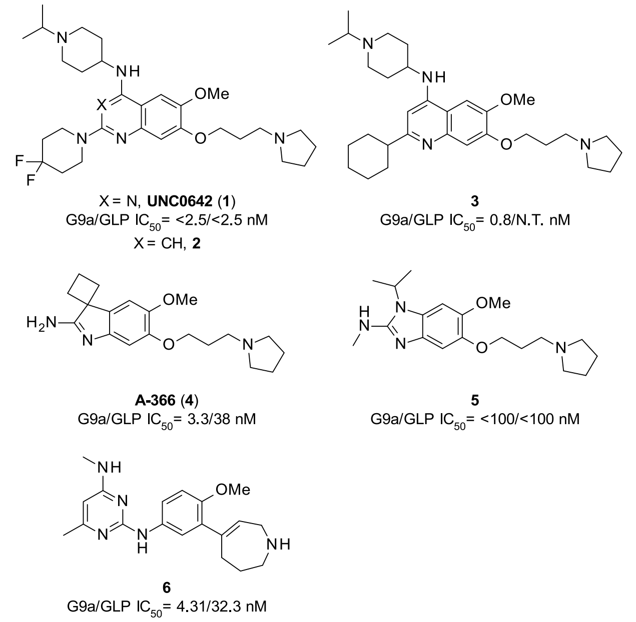

Figure 1. Chemical structures of select G9a/GLP inhibitors.

addition, several other chemotherapeutic agents for treating SCD have been developed. For instance, DNA methyltransferase inhibitors (such as 5-azacytidine and decitabine), histone deacetylase inhibitors (such as butyrate and panobinostat), and antidiabetic drugs (such as metformin) have been used to successfully induce HbF production via different mechanisms in preclinical studies.[11] The proof of concept for the therapeutic effects of many of these agents in these diseases has been demonstrated, but such agents need to be improved in terms of safety and efficacy; these issues must be overcome before or during clinical trials.

Recent reports have shown that individual genetic knockdown of G9a or GLP, which are histone methyltransferases (HMTs), induced HbF production.[12,13] Therefore, the development of potent dual G9a/GLP inhibitors that can induce HbF production could represent a refined and targeted approach for treating β-thalassemia and SCD. Actually, Epizyme Inc. developed EZM8266 (structure not disclosed), which is an orally available G9a inhibitor, for the treatment of SCD.[14]

To date, several classes of structurally diverse G9a/GLP inhibitors have been reported (Figure 1).[15] Representative examples are UNC0642 (**1**), which was the first *in vivo* chemical probe of G9a/GLP,[16] and quinoline derivative **3**, which shows strong *in vitro* potency.[17] Moreover, completely distinct classes of compounds that inhibit G9a/GLP have been identified, such as aminoindole A-366 (**4**)[18] and 2-aminobenzimidazole (**5**).[19] We previously reported the discovery of a novel potent G9a/GLP inhibitor (**6**) with a fixed cyclic side chain.[20] Here, we report on our efforts to further develop this inhibitor to increase its potency and to improve its absorption, distribution, metabolism, excretion, and toxicity (ADMET) properties to exhibit *in vivo* efficacy at a low predicted dose.

In the above-mentioned report,[20] we described the discovery of the tetrahydroazepine side chain as a novel motif for a Lys binding site, where a 3-(pyrrolidin-1-yl)propoxy group had usually been used. To examine the versatility of this side chain, we introduced it to the other central cores of known G9a/GLP inhibitor series (Table 1). First, based on the activity results of compounds **1** and **3**, we decided to synthesize quinoline derivative **7**,[21] which, as expected, showed more potent activity than compound **6** (IC_{50} = 2.00 nM for G9a, 6.15 nM for GLP). Next, indole derivative **8**, in which tetrahydroazepine was introduced into indole-based A-366, retained the potency.

Table 1. Chemical Structures, Activity, ADMET Profiles, and PK Profiles of Tetrahydroazepine Derivatives

Compound	**6**	**7**	**8**	**9**
Structure	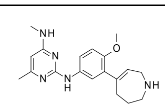	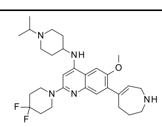	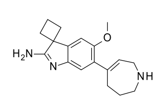	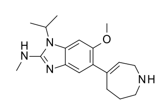
G9a IC_{50}[a] (nM)	4.31 ± 0.179	2.00 ± 0.0496	4.50 ± 0.155	22.8 ± 1.71
GLP IC_{50}[a] (nM)	32.3 ± 1.10	6.15 ± 0.366	33.9 ± 2.57	390 ± 34.4
log *D* (pH = 7.4)	0.5	0.3	−0.8	−0.3
MDCK Papp (10^{-6} cm/s)	1.4	0.23	2.7	0.6
MS % (human/monkey/mouse)	96/24/34	87/72/88	99/47/95	98/92/63
hERG inhibition (1/3/10/30 μM)	2/−1/1/23	N.T.[b]	5/6/5/5	8/2/3/8
PK parameters (mouse: 10 mg/kg, p.o.)				
C_{max} (μM)	0.45	0.02	0.04	0.03
AUC_{inf} (μM*h)	3.15	0.02	0.64	0.16
BA %	40	N.T.[b]	4.5	1.6

[a]The IC_{50} values are presented as the mean of four technical replicates ± the standard error of the mean (SEM). [b]Not tested.

https://dx.doi.org/10.1021/acsmedchemlett.0c00572
ACS Med. Chem. Lett. 2021, 12, 121−128

Table 2. Structure–Activity Relationships of Indole Derivatives

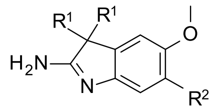

Compound	R^1	R^2	G9a IC_{50}[a] (nM)	GLP IC_{50}[a] (nM)
8		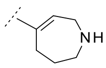	4.50 ± 0.155	33.9 ± 2.57
10 (DS79932728)		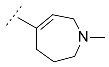	12.6 ± 0.228	75.7 ± 2.21
11		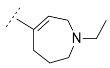	3.13 ± 0.178	20.3 ± 0.765
12		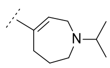	8.57 ± 0.426	61.6 ± 2.51
13		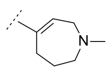	32.0 ± 1.45	155 ± 4.80
14	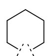	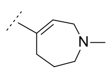	172 ± 11.2	1057 ± 67.8
15	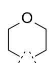	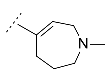	719 ± 54.4	3491 ± 143
16		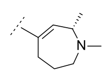	2148 ± 93.3	>5000
17		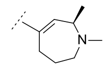	353 ± 18.7	2174 ± 126
18		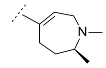	20.7 ± 0.559	85.5 ± 2.19
19		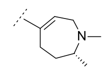	102 ± 3.83	205 ± 7.05
20		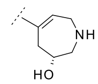	155 ± 16.5	1424 ± 78.4
21		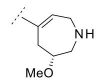	2331 ± 99.8	>5000
22		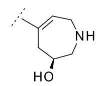	34.6 ± 2.70	385 ± 21.6
23		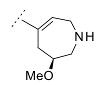	3151 ± 142	>5000

[a]The IC_{50} values are presented as the mean of four technical replicates ± the standard error of the mean (SEM).

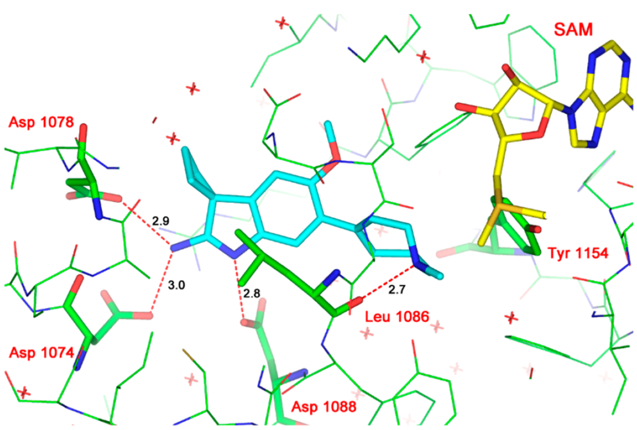

Figure 2. X-ray crystal structure of compound **10** bound to G9a (PDB code 7DCF).

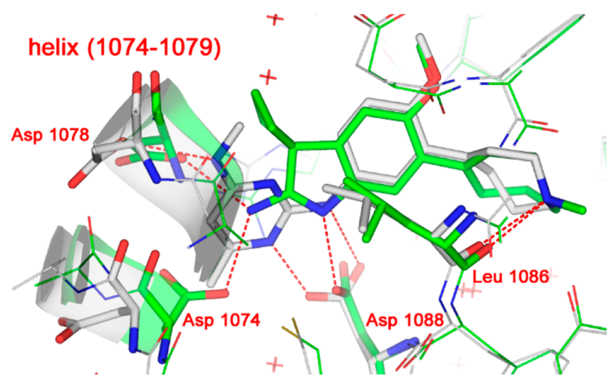

Figure 3. Overlay of the X-ray crystal structures of compounds **6** (gray, PDB code: 7BUC) and **10** (green, PDB code: 7DCF) bound to G9a.

Finally, benzimidazole derivative **9**, in which tetrahydroazepine was introduced into a known benzimidazole-based G9a/GLP inhibitor,[19] resulted in a 5-fold decrease in potency compared with compound **6** but still showed an IC_{50} value of 22.8 nM for G9a. These results indicated that the tetrahydroazepine side chain had versatility in terms of activity through the various central cores.

Based on the activity and ADMET profile results (in particular, membrane permeability and metabolic stability), we focused on the indole scaffold and attempted to find novel compounds in this series with improved pharmacokinetics (PK) profiles while maintaining G9a/GLP inhibitory activity. Incidentally, because the activity values of G9a and GLP were well correlated (Figure S1), we focus on G9a activity hereafter.

We explored the structure–activity relationships (SARs) of indole derivatives (Table 2). The initial SAR evaluation was

https://dx.doi.org/10.1021/acsmedchemlett.0c00572
ACS Med. Chem. Lett. 2021, 12, 121–128

Table 3. Physicochemical Properties and ADMET Profiles of Compounds 8, 10, and 11

compound	Log *D* (pH = 7.4)	solubility[a] (μg/mL) (JP1/JP2)	MDCK Papp (10^{-6} cm/s)	MS[b] (m/mon/h)	CYP direct inhibition[c]	MBI[d]	hERG inhibition[e]	Ames assays[f]	rat hepatocyte toxicity (IC_{50})
8	−0.8	590/590	2.7	47/95/99	0/0/0/2/0/1	82	5/6/5/5	N.T.[g]	N.T.[g]
10	−0.1	620/600	0.8	21/79/98	7/4/8/5/4/10	94	−6/−9/−6/1	negative	>300 μM
11	0.1	>650/>650	0.6	14/86/95	0/0/0/0/0/1	90	4/4/8/16	N.T.[g]	N.T.[g]

[a]JP1/JP2: Japanese Pharmacopoeia first/second test fluid (pH = 1.2/6.8). [b]The percentage (%) of the tested compound remaining after 0.5 h of incubation with mouse/monkey/human liver microsomes (0.5 mg/mL). [c]The percentage (%) inhibition of 1A2/2C8/2C9/2C19/2D6/3A4 at 10 μM. [d]The percentage (%) remaining at a concentration of 100 μM of compound reacted with CYP3A4 probe substrates after 30 min of preincubation in human liver microsomes. [e]The percentage (%) inhibition at 1/3/10/30 μM. [f]Ames assays were performed up to 1000 μg/well with or without S9 using *Salmonella* TA98 and TA100. [g]Not tested.

Table 4. Mouse Pharmacokinetics Profiles of Compounds 8, 10, and 11

	PO[a] (10 mg/kg; *n* = 2)				IV[b] (1 mg/kg; *n* = 2)				
compound	C_{max} (μM)	AUC_{inf} (μM·h)	T_{max} (h)	BA (%)	C_0 (μM)	AUC_{inf} (μM·h)	$T_{1/2}$ (h)	Vd_{ss} (L/kg)	CL_{inf} (mL/min/kg)
8	0.04	0.64	3.75	4.5	2.4	1.4	21.1	36.5	39.4
10	0.44	12.0	1.5	96	1.5	1.2	11.9	31.1	43.8
11	0.51	3.6	1.00	11	1.3	3.4	13.9	14.7	15.0

[a]Dosing vehicle: 0.5% methylcellulose (MC) solution. [b]Dosing vehicle: DMA/Tween80/saline = 10/10/80.

Table 5. Monkey Pharmacokinetics Profile of Compound 10

	PO[a] (5 mg/kg; *n* = 2)				IV[b] (0.5 mg/kg; *n* = 2)				
compound	C_{max} (μM)	AUC_{inf} (μM·h)	T_{max} (h)	BA (%)	C_0 (μM)	AUC_{inf} (μM·h)	$T_{1/2}$ (h)	Vd_{ss} (L)	CL_{inf} (mL/min/kg)
10	0.11	1.36	3.00	38	0.86	0.35	22.7	109	77.7

[a]Dosing vehicle: 0.5% MC solution. [b]Dosing vehicle: DMA/Tween80/saline = 10/10/80

directed toward modifications of *N*-substituents at the tetrahydroazepine ring. When the substituent on the *N* of the tetrahydroazepine ring was transformed, the ethyl group (**11**) retained activity, while the methyl group (**10**) showed a 3-fold decrease in activity and the isopropyl group (**12**) showed a 2-fold decrease in activity. Replacing the cyclobutyl group of compound **10** with cyclopentyl (**13**) and cyclohexyl (**14**) groups conferred much lower potency (IC_{50} = 32 and 172 nM for G9a, respectively). These potency results corresponded with those of the A-366 series,[18] suggesting that these derivatives bind to the same G9a/GLP protein site as A-366. Likewise, the tetrahydropyranyl group derivative **15** resulted in a loss of potency. Next, to obtain further SARs and improve the activity, a methyl group was introduced at the *α* position of the tetrahydroazepine ring (**16**−**19**), which led to a decrease in activity. In addition, the introduction of a hydroxy or methoxy group at the *β* position of the tetrahydroazepine ring (**20**−**23**) resulted in reduced activity. The description of these activity results based on the cocrystal structure is described later.

To determine the binding mode of the newly synthesized inhibitors, we solved the X-ray cocrystal structure of compound **10** with G9a (Figure 2). The cocrystal structure of compound **10** with G9a revealed the same binding site as that previously reported for A-366;[18] thus, the mechanism of action of inhibitor **10** was expected to show a noncompetitive inhibition pattern against the cofactor S-adenosyl methionine. The hydrogen bonding patterns revealed interactions between the side chain of Leu1086, the amino group of tetrahydroazepine, and the side chains of Asp1078, Asp1088, Asp1074, and the amidine group. These findings are similar to those found for A-366.

Next, the activity results of compounds **16**−**23** were examined based on this cocrystal structure. Compounds **16**, **17**, and **19** showed a significant reduction in activity, likely due to steric repulsion with Y1154. Only compound **18** showed retained activity, likely due to low steric repulsion. Further, the activity of methoxy derivatives **21** and **23** was greatly decreased, likely due to steric repulsion with Y1154. In contrast, the hydroxy group in compounds **20** and **22** appeared to form hydrogen bonds with the main chain carbonyl group of Y1154, and especially the hydrogen bond angle of compound **22** would be better than compound **20**, which led to retain the activity.

In the comparison of the cocrystal structures of compound **10** and the previously reported compound **6** (Figure 3), the tetrahydroazepine moiety of each inhibitor was found to be located at approximately the same position and was hydrogen-bonded to the side chain of Leu1086. In contrast, the helix (1074−1079) was slightly off, and in the case of compound **10**, it was closer to the inhibitor. Considering the difference of the molecular size of each inhibitor, it seems that the conserved interaction of the tetrahydroazepine moiety with Leu1086 controls the location of the inhibitor in the active sites of enzymes. As a result, the interaction patterns with the helix (1074−1079) are different between the inhibitors. Namely, the primary amino group of compound **10** characteristically forms hydrogen bonds with the side chains of Asp1078 and Asp1074, whereas the amino moiety of compound **6** forms hydrogen bonds with only the side chain of Asp 1078, not Asp1074. In addition, with respect to the interaction with Asp1088, aminopyrimidine (**6**) forms a hydrogen bond and salt-bridge, while the indole nitrogen of compound **10** only forms a salt-bridge with Asp1088.

The physicochemical properties and ADMET profiles of representative compounds **8**, **10**, and **11** are summarized in Table 3. These compounds showed low log *D* values, high solubility, and high metabolic stability in both monkey and human liver microsomes. These compounds did not exhibit CYP inhibitory activity at a concentration of 10 μM, and they also did not exhibit mechanism-based inhibition (MBI) of

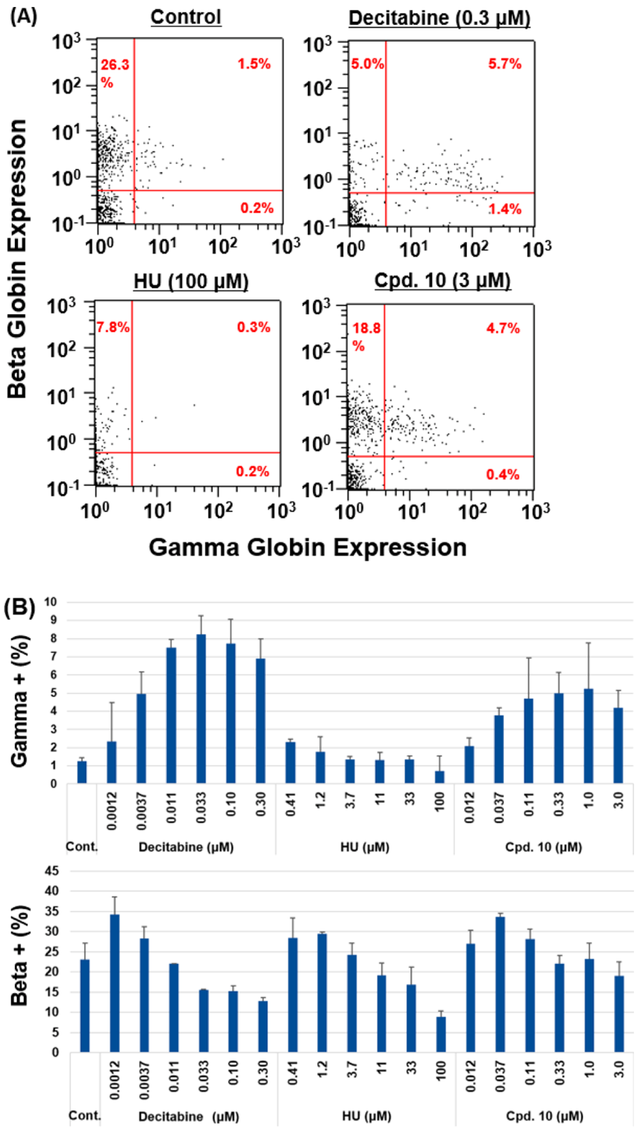

Figure 4. Assessment (F-cell; flow cytometry [FCM]) of *in vitro* activity of decitabine, hydroxyurea (HU), and compound **10** using cynomolgus monkey bone marrow mononuclear cells. (A) γ-Globin and β-globin levels in the cells were evaluated by FCM. Representative FCM plots of each compound are shown. (B) The percentage of γ-globin- and β-globin-positive cells at each concentration of the compounds is shown. Data are expressed as the mean ± the standard deviation of the three biological replicates.

CYP3A4. Furthermore, these compounds showed low human ether-a-go-go-related gene (hERG) inhibition at concentrations up to 30 μM and improved inhibition compared to compound **6** (23% at 30 μM). Mouse PK parameters of compounds **8**, **10**, and **11** are summarized in Table 4. Although compound **8** showed the highest C_0 with intravenous (IV) administration of these compounds, plasma exposure with oral administration was worse, and the bioavailability (BA) of **8** was the lowest of the three compounds. Compound **10** showed the highest AUC_{inf} with oral administration and the highest BA, despite its moderate-to-high CL_{inf}. Compound **11** had a low CL_{inf} with IV administration, and with oral exposure, it was lower than that of compound **10**. Thus, we selected compound **10** for monkey PK studies because of its high AUC_{inf} and good oral BA in mice (BA = 96%).

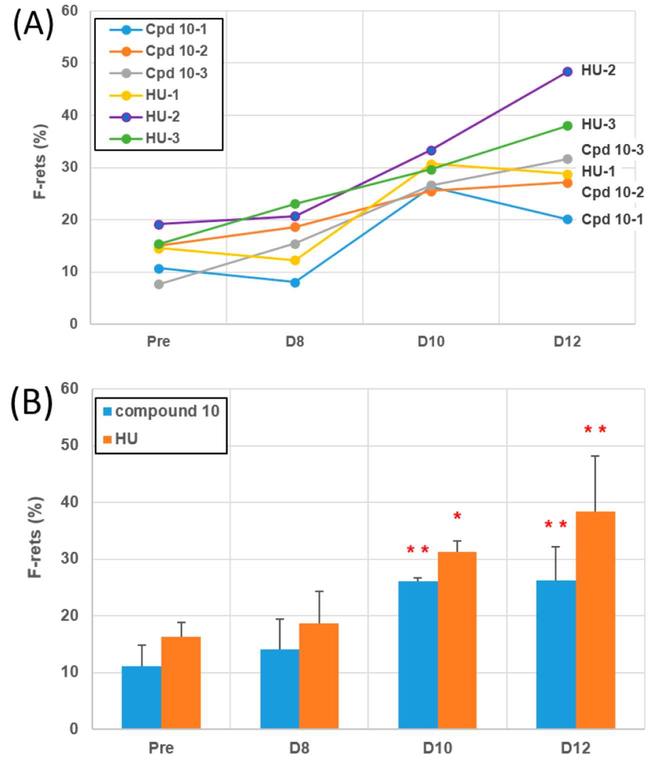

Figure 5. Efficacy of compound **10** and HU on F-reticulocytes (F-rets) per flow cytometry. (A) Individual monkey data on the rate of change in F-rets before administration (pretreatment) and on days 8, 10, and 12. (B) Average rate of change in F-rets in the HU and compound **10** groups. Three-year-old male cynomolgus monkeys were phlebotomized three times a week to establish an anemia model in which their blood hemoglobin levels were below 10.5 g/dL. Compound **10** was orally administered twice daily to three monkeys (Cpd 10-1, Cpd 10-2, and Cpd 10-3) at a dose of 15 mg/kg from Day 1 to Day 5. HU was orally administered once daily to three monkeys (HU-1, HU-2, and HU-3) at a dose of 35 mg/kg from Day 1 to Day 5. F-rets were measured 3 days before dose initiation (pretreatment) and on days 8, 10, and 12. F-ret data for each treatment group are expressed as the mean ± the standard deviation of the three monkeys. * $P < 0.05$ and ** $P < 0.01$ indicate statistically significant differences compared with each pretreatment group.

Table 5 shows the monkey PK profile of compound **10**. In this study, compound **10** exhibited high plasma exposure, and we confirmed that it had a suitable profile for *in vivo* monkey pharmacodynamics studies with oral administration. Prior to *in vivo* study, we confirmed the cellular activity of the representative compound (**10**). To determine the HbF production-inducing activity of compound **10**, decitabine, and HU, *in vitro* activity assessment (F-cell; flow cytometry [FCM]) was performed using a cellular system with cynomolgus monkey bone marrow mononuclear cells (Figure 4). As decitabine enhances HbF production in cynomolgus monkey bone marrow mononuclear cells,[22] it was used as a positive control to validate the experimental procedure. As expected, concentration-dependent increases in the rate of γ-globin-positive cells were observed with decitabine and compound **10**, suggesting that compound **10** could induce HbF production similar to decitabine in cynomolgus monkey bone marrow mononuclear cells. In contrast, no increase in the rate of γ-globin-positive cells was observed for HU. Furthermore, in comparison with decitabine and HU, the effect of compound **10** in terms of the reduction of β-globin-positive cells was relatively mild,

https://dx.doi.org/10.1021/acsmedchemlett.0c00572
ACS Med. Chem. Lett. 2021, 12, 121−128

Scheme 1. Synthesis of Compound 10[a]

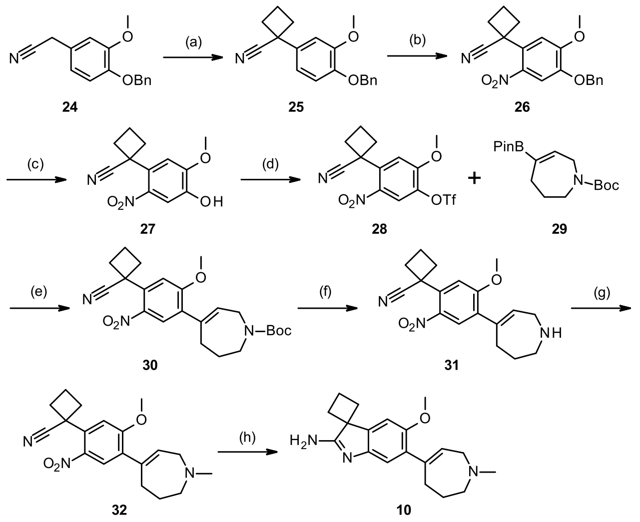

[a]Reagents and conditions: (a) 1,3-dibromopropane, NaH, DMF, 0 °C to rt, 1 h, 67%; (b) HNO_3, Ac_2O, AcOH, 0 °C, 30 min, 59%; (c) 10% Pd/C, 1,4-cyclohexadiene, EtOH, AcOEt, rt to 80 °C, 30 min; (d) Tf_2O, Et_3N, CH_2Cl_2, 0 °C, 30 min, 72% over 2 steps; (e) $Pd(dppf)Cl_2$, K_2CO_3, dioxane, H_2O, μW, 120 °C, 1 h, 93%; (f) TFA, CH_2Cl_2, rt, 30 min, 95%; (g) formaldehyde, $NaBH(OAc)_3$, AcOH, CH_2Cl_2, rt, 1 h, 94%; (h) Zn, AcOH, THF, 40 °C, 5 min; H_2, 10% Pd/C, Ac_2O, THF, rt, 20 min, 61% over 2 steps.

suggesting that compound **10** would not drastically inhibit the proliferation and differentiation of erythrocytes and is likely to be much safer than decitabine and HU. Next, we tested the cellular activity of the representative compound (**10**) by evaluating the switching of globin mRNA expression from adult-type β-globin to fetal-type γ-globin using human cultured bone marrow CD34+ cells (Figure S2).[23] The cellular globin switching activity of compound **10** was almost the same as that of compound **4**, suggesting that compound **10** has activity not only in monkey cells, but also in human cells.

Based on the above findings, we tested the effects of the compounds in nonhuman primates, which are considered to be the best animal model to study the effects of HbF production-inducing drugs due to the conservation of the pattern of developmental expression of β-like globin genes.[24−28] Compound **10** was evaluated for its ability to induce γ-globin production *in vivo* using a phlebotomized cynomolgus monkey model with HU as a control (Figure 5). To confirm the induction of γ-globin production, F-reticulocyte (F-ret) values (reticulocytes exhibiting γ-globin) were analyzed by FCM using phlebotomized cynomolgus monkeys. The results showed that compound **10** (15 mg/kg bid) induced F-rets at almost the same exposure as that of the simulation (assuming exposure of C_{max} = 0.3 μM; Figure S3). Compound **10** also performed comparably to HU in this model (35 mg/kg and qd, which is equivalent to the highest dose used clinically for SCD treatment based on plasma exposure). Throughout the *in vivo* experiments, no safety issues, including myelosuppression, were observed (Figure S4). To the best of our knowledge, compound **10** is the first G9a/GLP inhibitor to show the induction of γ-globin production in a cynomolgus monkey model.

The preparation of representative compound **10** is shown in Scheme 1. Commencing with phenylacetonitrile (**24**), dialkylation of the benzylic carbon with dibromopropane led to compound **25**. Subsequent regioselective nitration with nitric acid followed by removal of the benzyl group using Pd/C and cyclohexadiene afforded compound **27**. Triflation of compound **27** followed by Suzuki-Miyaura coupling with boronic acid pinacol ester (**29**)[20] afforded compound **30**. Removal of the *tert*-butoxycarbonyl group under acidic conditions followed by *N*-methylation led to compound **32**. The formation of a spiro[cycloalkyl-1,3′-indol]-2′-amine core was achieved by reductive cyclization. Initially, we attempted to obtain compound **10** by using the conditions reported by Sweis et al. (H_2; 10% Pd/C; acetic acid, or Zn; acetic acid),[18] but in this case, the yield was low because of low conversion. Therefore, we optimized the conditions and finally constructed a spiro-[cycloalkyl-1,3′-indol]-2′-amine core by reduction of the nitro group with Zn in acetic acid followed by 10% Pd/C under an atmosphere of hydrogen in Ac_2O and tetrahydrofuran, which afforded compound **10**.

In conclusion, we successfully identified spiro[cycloalkyl-1,3-indol]-2′-amine derivatives as G9a/GLP inhibitors. In the course of our exploration of G9a/GLP inhibitors that are more potent and have improved PK profiles compared to existing G9a/GLP inhibitors, it was found that the tetrahydroazepine side chain that we originally discovered could be applied for various types of central cores of known G9a/GLP inhibitors. Among these inhibitors, we synthesized and evaluated a series of spiro[cycloalkyl-1,3′-indol]-2′-amine derivatives, and ultimately compound **10** (DS79932728) was identified as a promising compound. DS79932728 showed excellent metabolic stability in monkeys, and we confirmed that it was sufficiently exposed through monkey PK tests (BA = 38%). In the *in vivo* phlebotomized cynomolgus monkey model, DS79932728, showed γ-globin induction at 15 mg/kg p.o., and the effect of DS79932728 on HbF levels appeared to be comparable to that of HU. Because there are only a handful of reports of small molecules showing the induction of γ-globin production in a monkey model,[29−34] DS79932728 is expected to be useful for studying the treatment of β-thalassemia and SCD.

■ ASSOCIATED CONTENT

Supporting Information

The Supporting Information is available free of charge at https://pubs.acs.org/doi/10.1021/acsmedchemlett.0c00572.

Details on the preparation of compounds **1−23** (including synthetic procedures), *in vitro* assays, *in vivo* assays, and X-ray crystallography (PDF)

■ AUTHOR INFORMATION

Corresponding Authors

Katsushi Katayama − *R&D Division, Daiichi Sankyo Co., Ltd., Shinagawa-ku, Tokyo 140-8710, Japan;* orcid.org/0000-0003-1876-7974; Email: katayama.katsushi.ne@daiichisankyo.co.jp

Takahiro Katagiri − *R&D Division, Daiichi Sankyo Co., Ltd., Shinagawa-ku, Tokyo 140-8710, Japan;* Email: katagiri.takahiro.k6@daiichisankyo.co.jp

Authors

Ken Ishii − *R&D Division, Daiichi Sankyo Co., Ltd., Shinagawa-ku, Tokyo 140-8710, Japan*

Hideki Terashima − *R&D Division, Daiichi Sankyo Co., Ltd., Shinagawa-ku, Tokyo 140-8710, Japan*

Eisuke Tsuda − *R&D Division, Daiichi Sankyo Co., Ltd., Shinagawa-ku, Tokyo 140-8710, Japan*

https://dx.doi.org/10.1021/acsmedchemlett.0c00572
ACS Med. Chem. Lett. 2021, 12, 121−128

Makoto Suzuki − *Daiichi Sankyo RD Novare Co., Ltd., Edogawa-ku, Tokyo 134-8630, Japan*
Keiichi Yotsumoto − *R&D Division, Daiichi Sankyo Co., Ltd., Shinagawa-ku, Tokyo 140-8710, Japan*
Kumiko Hiramoto − *Daiichi Sankyo RD Novare Co., Ltd., Edogawa-ku, Tokyo 134-8630, Japan*
Isao Yasumatsu − *Daiichi Sankyo RD Novare Co., Ltd., Shinagawa-ku, Tokyo 140-8710, Japan*
Munefumi Torihata − *R&D Division, Daiichi Sankyo Co., Ltd., Shinagawa-ku, Tokyo 140-8710, Japan*
Takashi Ishiyama − *R&D Division, Daiichi Sankyo Co., Ltd., Shinagawa-ku, Tokyo 140-8710, Japan*
Tsuyoshi Muto − *R&D Division, Daiichi Sankyo Co., Ltd., Shinagawa-ku, Tokyo 140-8710, Japan*

Complete contact information is available at:
https://pubs.acs.org/10.1021/acsmedchemlett.0c00572

Notes

The authors declare no competing financial interest.

■ ACKNOWLEDGMENTS

We thank Dr. Naoki Tanaka for helpful discussions on medicinal chemistry and manuscript preparation. We appreciate Mr. Tadayoshi Mizuno and Ms. Tomoko Yoneyama for G9a protein production and purification.

■ ABBREVIATIONS

SCD sickle cell disease
RBC red blood cell
HbS sickle hemoglobin
HbA adult hemoglobin
HbF fetal hemoglobin
HU hydroxyurea
FDA Food and Drug Administration
ADMET absorption, distribution, metabolism, excretion, and toxicity
PK pharmacokinetics
IV intravenous
HERG human ether-a-go-go-related gene
FCM flow cytometry
DMF *N*,*N*-dimethylformamide
Boc *tert*-butoxycarbonyl
TFA trifluoroacetic acid
THF tetrahydrofuran
SAR structure−activity relationship
BA bioavailability
MDCK Madin−Darby canine kidney
MS metabolic stability
Pd/C palladium on carbon

■ REFERENCES

(1) Forget, B. G.; Bunn, H. F. Classification of the Disorders of Hemoglobin. *Cold Spring Harbor Perspect. Med.* **2013**, *3*, a011684.
(2) Galanello, R.; Origa, R. Beta-thalassemia. *Orphanet. J. Rare Diseases* **2010**, *5*, 11.
(3) Weatherall, D. J. The Inherited Diseases of Hemoglobin Are an Emerging Global Health Burden. *Blood* **2010**, *115*, 4331−4336.
(4) Borgna-Pignatti, C. The Life of Patients with Thalassemia Major. *Haematologica* **2010**, *95*, 345−348.
(5) Wilber, A.; Nienhuis, A. W.; Persons, D. A. Transcriptional Regulation of Fetal to Adult Hemoglobin Switching: New Therapeutic Opportunities. *Blood* **2011**, *117*, 3945−3953.
(6) Perrine, S. P.; Pace, B. S.; Faller, D. V. Targeted Fetal Hemoglobin Induction for Treatment of Beta Hemoglobinopathies. *Hematol. Oncol. Clin. North Am.* **2014**, *28*, 233−248.
(7) Ware, R. E.; Aygun, B. Advances in the Use of Hydroxyurea. *Am. Soc. Hematol. Educ. Program* **2009**, *1*, 62−69.
(8) Testa, U. Fetal Hemoglobin Chemical Inducers for Treatment of Hemoglobinopathies. *Ann. Hematol.* **2009**, *88*, 505−528.
(9) Steinberg, M. H.; McCarthy, W. F.; Castro, O.; Ballas, S. K.; Armstrong, F. D.; Smith, W.; Ataga, K.; Swerdlow, P.; Kutlar, A.; DeCastro, L.; Waclawiw, M. A. The Risks and Benefits of Long-Term Use of Hydroxyurea in Sickle Cell Anemia: A 17.5 Year Follow-up. *Am. J. Hematol.* **2010**, *85*, 403−408.
(10) Eaton, W. A.; Bunn, F. Treating Sickle Cell Disease by Targeting HbS Polymerization. *Blood* **2017**, *129*, 2719−2726.
(11) Paikari, A.; Sheehan, V. A. Fetal Haemoglobin Induction in Sickle Cell Disease. *Br. J. Haematol.* **2018**, *180*, 189−200.
(12) Krivega, I.; Byrnes, C.; de Vasconcellos, J. F.; Lee, Y. T.; Kaushal, M.; Dean, A.; Miller, J. L. Inhibition of G9a Methyltransferase Stimulates Fetal Hemoglobin Production by Facilitating LCR/γ-Globin Looping. *Blood* **2015**, *126*, 665−672.
(13) Renneville, A.; Van Galen, P.; Canver, M. C.; McConkey, M.; Krill-Burger, J. M.; Dorfman, D. M.; Holson, E. B.; Bernstein, B. E.; Orkin, S. H.; Bauer, D. E.; Ebert, B. L. EHMT1 and EHMT2 Inhibition Induces Fetal Hemoglobin Expression. *Blood* **2015**, *126*, 1930−1939.
(14) Epizyme developed EZM8266, but the preclinical studies were stopped due to toxicology study results. https://epizyme.gcs-web.com/news-releases/news-release-details/epizyme-announces-positive-pre-nda-meeting-tazemetostat. (accessed Oct 20, 2020).
(15) Cao, H.; Li, L.; Yang, D.; Zeng, L.; Yewei, X.; Yu, B.; Liao, G.; Chen, J. Recent Progress in Histone Methyltransferase (G9a) Inhibitors as Anticancer Agents. *Eur. J. Med. Chem.* **2019**, *179*, 537−546.
(16) Liu, F.; Barsyte-Lovejoy, D.; Li, F.; Xiong, Y.; Korboukh, V.; Huang, X.; Allali-Hassani, A.; Janzen, W. P.; Roth, B. L.; Frye, S. V.; Arrowsmith, C. H.; Brown, P. J.; Vedadi, M.; Jin, J. Discovery of an In Vivo Chemical Probe of the Lysine Methyltransferases G9a and GLP. *J. Med. Chem.* **2013**, *56*, 8931−8942.
(17) Rabal, O.; José-Enériz, E. S.; Agirre, X.; Sánchez-Arias, J. A.; Vilas-Zornoza, A.; Ugarte, A.; Miguel, I.; Miranda, E.; Garate, L.; Fraga, M.; Santamarina, P.; Perez, R. F.; Ordoñez, R.; Sáez, E.; Roa, S.; García-Barchino, M. J.; Martínez-Climent, J. A.; Liu, Y.; Wu, W.; Xu, M.; Prosper, F.; Oyarzabal, J. Discovery of Reversible DNA Methyltransferase and Lysine Methyltransferase G9a Inhibitors with Antitumoral In Vivo Efficacy. *J. Med. Chem.* **2018**, *61*, 6518−6545.
(18) Sweis, R. F.; Pliushchev, M.; Brown, P. J.; Guo, J.; Li, F.; Maag, D.; Petros, A. M.; Soni, N. B.; Tse, C.; Vedadi, M.; Michaelides, M. R.; Chiang, G. G.; Pappano, W. N. Discovery and Development of Potent and Selective Inhibitors of Histone Methyltransferase G9a. *ACS Med. Chem. Lett.* **2014**, *5*, 205−209.
(19) Campbell, J. E.; Duncan, K. W. Preparation of Substituted Fused Bi- or Tri-Heterocyclic Compounds as EHMT2 Inhibitors. WO 2018064557, April 5, 2018.
(20) Katayama, K.; Ishii, K.; Tsuda, E.; Yotsumoto, K.; Hiramoto, K.; Suzuki, M.; Yasumatsu, I.; Igarashi, W.; Torihata, M.; Ishiyama, T.; Katagiri, T. Discovery of Novel Histone Lysine Methyltransferase G9a/GLP (EHMT2/1) Inhibitors: Design, Synthesis, and Structure-Activity Relationships of 2,4-Diamino-6-Methylpyrimidines. *Bioorg. Med. Chem. Lett.* **2020**, *30*, 127475.
(21) Before the synthesis development of tetrahydroazepine derivatives, considering the result of the activity of compound **3**, quinoline **2** in which the 3-position of compound **1** was converted from N to CH was first synthesized and found to be more potent than quinazoline **1** (data not shown).
(22) Lavelle, D.; Saunthararajah, Y.; Vaitkus, K.; Singh, M.; Banzon, V.; Phiasivongsva, P.; Redkar, S.; Kanekal, S.; Bearss, D.; Shi, C.; Inloes, R.; DeSimone, J. S110, a Novel Decitabine Dinucleotide, Increases Fetal Hemoglobin Levels in Baboons (*P. anubis*). *J. Transl. Med.* **2010**, *8*, 92.

(23) Lee, Y.; Vasconcellos, J. F.; Yuan, J.; Byrnes, C.; Noh, S. J.; Meier, E. R.; Kim, K. S.; Rabel, A.; Kaushal, M.; Muljo, S. A.; Miller, J. L. LIN28B-Mediated Expression of Fetal Hemoglobin and Production of Fetal-Like Erythrocytes from Adult Human Erythroblasts Ex Vivo. *Blood* **2013**, *122*, 1034−1041.

(24) In general, transgenic mice with the human β-globin locus consisting of linked embryonic (ε), fetal (γ), and adult (β) genes are systems for investigating the transient fetal to adult hemoglobin switching as occurs in humans. However, it has been reported that the human γ-globin in these mice behaves as murine embryonic globin genes; thus, there are limitations to confirming pharmacological efficacy in this model. Actually, HU is essentially ineffective at inducing HbF in various transgenic mouse models of SCD. In contrast, it has been shown to reliably induce HbF in baboon or cynomolgus monkey models that retain hemoglobin switching.

(25) Sankaran, V. G.; Xu, J.; Ragoczy, T.; Ippolito, G. C.; Walkley, C. R.; Maika, S. D.; Fujiwara, Y.; Ito, M.; Groudine, M.; Bender, M. A.; Tucker, P. W.; Orkin, S. H. Developmental and Species-Divergent Globin Switching Are Driven by BCL11A. *Nature* **2009**, *460*, 1093−1097.

(26) Lebensburger, J. D.; Pestina, T. I.; Ware, R. E.; Boyd, K. L.; Persons, D. A. Hydroxyurea Therapy Requires HbF Induction for Clinical Benefit in a Sickle Cell Mouse Model. *Haematologica* **2010**, *95*, 1599−1603.

(27) Lavelle, D.; Molokie, R.; Ducksworth, J.; DeSimone, J. Effects of Hydroxurea, Stem Cell Factor, and Erythropoietin in Combination on Fetal Hemoglobin in the Baboon. *Exp. Hematol.* **2001**, *29*, 156−162.

(28) Kundu, M. C.; Gore, L. R.; Maguire, S.; Gilmartin, A. G. Development and Characterization of a Model for Inducing Fetal Hemoglobin Production in Cynomolgus Macaques (*Macaca fascicularis*). *Comp. Med.* **2018**, *68*, 396−402.

(29) Lavelle, D.; Chin, J.; Vaitkus, K.; Redkar, S.; Phiasivongsa, P.; Tang, C.; Will, R.; Hankewych, M.; Roxas, B.; Singh, M.; Saunthararajah, Y.; DeSimone, J. Oral Decitabine Reactivates Expression of the Methylated γ-Globin Gene in *Papio anubis*. *Am. J. Hematol.* **2007**, *82*, 981−985.

(30) Akpan, I.; Banzon, V.; Ibanez, V.; Vaitkus, K.; DeSimone, J.; Lavelle, D. Decitabine Increases Fetal Hemoglobin in *Papio anubis* by Increasing Gamma-Globin Gene Transcription. *Exp. Hematol.* **2010**, *38*, 989−993.

(31) Rivers, A.; Vaitkus, K.; Ibanez, V.; Ruiz, M. A.; Jagadeeswaran, R.; Saunthararajah, Y.; Cui, S.; Engel, J. D.; DeSimone, J.; Lavelle, D. The LSD1 Inhibitor RN-1 Recapitulates the Fetal Pattern of Hemoglobin Synthesis in Baboons (*P. anubis*). *Haemotologicia* **2016**, *101*, 688−697.

(32) Rivers, A.; Vaitkus, K.; Jagadeeswaran, R.; Ruiz, M. A.; Ibanez, V.; Ciceri, F.; Cavalcanti, F.; Molokie, R. E.; Saunthararajah, Y.; Engel, J. D.; DeSimone, J.; Lavelle, D. Oral Administration of the LSD1 Inhibitor ORY-3001 Increases Fetal Hemoglobin in Sickle Cell Mice and Baboons. *Exp. Hematol.* **2018**, *67*, 60−64.e2.

(33) Makino, T.; Haruyama, M.; Katayama, K.; Terashima, H.; Tsunemi, T.; Miyazaki, K.; Terakawa, M.; Yamashiro, K.; Yoshioka, R.; Maeda, H. Phenotypic-Screening Generates Active Novel Fetal Globin-Inducers that Downregulate Bcl11a in a Monkey Model. *Biochem. Pharmacol.* **2020**, *171*, 113717.

(34) Katayama, K.; Tsunemi, T.; Miyazaki, M.; Uoto, K.; Yoshioka, R.; Terashima, H.; Terakawa, M.; Yamashiro, K.; Haruyama, M.; Maeda, H.; Makino, T. Design, Synthesis, and Optimization of a Series of 2-Azaspiro[3.3]heptane Derivatives as Orally Bioavailable Fetal Hemoglobin Inducers. *Bioorg. Med. Chem. Lett.* **2020**, *30*, 127425.

https://dx.doi.org/10.1021/acsmedchemlett.0c00572
ACS Med. Chem. Lett. 2021, 12, 121−128